

Synthesis, structure and photochromism of zinc(II) complexes of alkylthioarylazoimidazoles

Shefali Saha (Halder)^a, Partha Mitra^b, Chittaranjan Sinha^{a,*}

^a Department of Chemistry, Inorganic Chemistry Section, Jadavpur University, Kolkata 700 032, India

^b Department of Inorganic Chemistry, Indian Association for the Cultivation of Science, Kolkata 700 032, India



ARTICLE INFO

Article history:

Received 18 July 2013

Accepted 2 September 2013

Available online 25 September 2013

Keywords:

Zn(II)-thioalkylphenyl-azoimidazole

Distorted Td-symmetry

Photochromism

Activation energy

Effect of halide

ABSTRACT

The $[Zn(SRaaiNR')(H_2O)X_2]$ ($SRaaiNR' = 1\text{-alkyl-}2\text{-}\{(\text{o-thioalkyl})\text{phenylazo}\}\text{imidazole}$; $X = \text{Cl}, \text{Br}, \text{I}$) complexes have been characterized by spectroscopic studies. The X-ray structure of $[Zn(SEtaaiNET)(H_2O)\text{Cl}_2]$ (where $SEtaaiNET = 1\text{-ethyl-}2\text{-}\{(\text{o-thioalkyl})\text{phenylazo}\}\text{imidazole}$) shows bidentate imidazolyl-N, azo-N chelation of $SEtaaiNET$ and the other donors are H_2O and 2Cl^- . UV light irradiation to a MeCN solution of the complexes shows E-to-Z (E and Z refer to *trans* and *cis*-configurations about $-\text{N}=\text{N}-$, respectively) isomerisation of the coordinated azoimidazole. The rate of isomerisation follows the sequence: $[Zn(SRaaiNR')(H_2O)\text{Cl}_2] < [Zn(SRaaiNR')(H_2O)\text{Br}_2] < [Zn(SRaaiNR')(H_2O)]_2$. The quantum yields ($\phi_{E \rightarrow Z}$) and the activation energies (E_a) of the isomerisation of the complexes are lower than those of the free ligands. The observation has been explained considering the molecular association that increases the mass and rotor volume of the complexes.

© 2013 Elsevier Ltd. All rights reserved.

1. Introduction

Zinc, the fourth most widely used metal after iron, aluminum and copper [1], is anticorrosive and is used to protect bridges, buildings etc. from loss through rusting. It is an essential trace element and more than 150 metalloenzymes are either directly or indirectly dependent on zinc(II) [2,3] and fight cancer [4]. DNA bases and other nucleotides and nucleosides strongly bind Zn(II). Imidazole and its derivatives form complexes of the type $[Zn(imzH)_6]\text{Cl}_2$ [5]. Imidazolato bridged Zn(II) complexes enhance the activity of Cu(II) in metallo-proteins [6,7]. Studies on Zn(II)-imidazole/imidazole containing ligands are of interest. This has prompted us to synthesize 1-alkyl-2-(arylazo)imidazoles (RaaiR') and investigate their coordination chemistry [8–13]. The molecules are π -acidic and the active function is an azoimine group ($-\text{N}=\text{N}-\text{C}=\text{N}-$). The coordination chemistry of Zn(II) with RaaiR' has recently been started by us [14–16]. One of the interesting properties of RaaiR' and many of their complexes is photochromism [17–20], which is a reversible transformation between E (*trans*) and Z (*cis*) isomers upon light irradiation. The photochromic compounds are applicable in different areas, such as liquid crystal alignment [21], optical data storage [22], non-linear optics [23], photoswitching [24] and molecular-photonics devices [25]. Very few azo compounds, including azobenzenes, arylazopyridines and arylazoimidazoles [17–25], show photochromic activity. This has stimulated us to functionalize RaaiR' for an investigation

of the effect of the substituents on the optical properties. We have synthesized 1-alkyl-2-(*o*-thioalkyl)phenylazo)imidazole (SRaaiNR') and their properties were examined [26,27]. In this work Zn(II)-SRaaiNR' complexes were structurally characterized and the light stimulated property of the coordinated SRaaiNR' has been examined. The effect of Zn-X (X = Cl, Br, I) on the photoisomerisation rate and quantum yields have been discussed.

2. Experimental

2.1. Material

Anhydrous ZnCl_2 , ZnBr_2 and ZnI_2 were obtained from Merck. 1-Alkyl-2-(*o*-thioalkyl) phenylazo)imidazole (SRaaiNR') were synthesized by a reported procedure [27]. All other chemicals and solvents were of reagent grade and used as received.

2.2. Physical measurements

Microanalytical data (C, H, N) were collected on Perkin-Elmer 2400 CHNS/O elemental analyzer. Spectroscopic data were obtained using the following instruments: UV-Vis spectra from a Perkin Elmer Lambda 25 spectrophotometer; IR spectra (KBr disk, 4000–200 cm^{-1}) from a Perkin Elmer RX-1 FTIR spectrophotometer; photoexcitation has been carried out using a Perkin Elmer LS-55 spectrophotometer and ^1H NMR spectra were collected on a Bruker (AC) 300 MHz FTNMR spectrometer.

* Corresponding author. Tel.: +91 9433621872; fax: +91 2414 6584.

E-mail address: c_r_sinha@yahoo.com (C. Sinha).

2.3. Synthesis

2.3.1. Synthesis of $[Zn(SMeaaiNMe)(H_2O)Cl_2]$ (3a)

To a methanol solution of 1-methyl-2-[(o-thiomethyl)phenylazo]imidazole (*SMeaaiNMe*) (52 mg, 0.23 mmol), a $ZnCl_2$ (30 mg, 0.22 mmol) solution (5 ml in MeOH) was added in drops and stirred for 2 h. The resultant reddish solution was then collected by filtration. Slow evaporation of the solution gives orange-red crystals. The yield was 52 mg (61%).

Other complexes were prepared under identical conditions from MeOH solution and the yields were 60–70%.

Microanalytical data of the complexes are as follows: $[Zn(SMeaaiNMe)(H_2O)Cl_2]$ (3a). Anal. Calc. for $ZnC_{11}H_{14}N_4OSCl_2$: C, 34.17; H, 3.62; N, 14.50. Found: C, 34.21; H, 3.60; N, 14.43%. FT-IR (KBr disc, cm^{-1}): $\nu(\text{N}=\text{N})$, 1424; $\nu(\text{C}=\text{N})$, 1622. UV-Vis spectroscopic data in CH_3CN (λ_{\max} (nm) ($10^{-3} \epsilon$ ($\text{dm}^3 \text{mol}^{-1} \text{cm}^{-1}$))): 362 (11.5), 416

Table 1
Summarized crystallographic data for $[Zn(SMeaaiNMe)(H_2O)Cl_2]$ (3a).

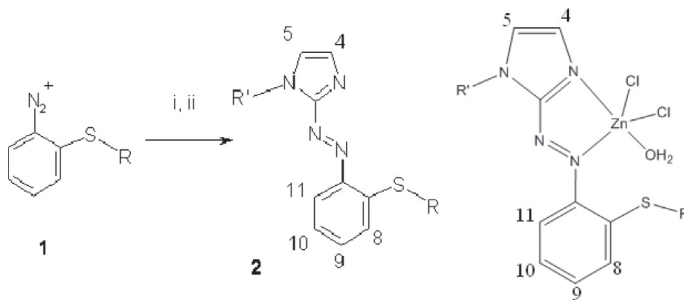
	$[Zn(SMeaaiNMe)(H_2O)Cl_2]$ (3a)
Empirical formula	$C_{11}H_{14}N_4OSCl_2Zn$
Formula weight	386.59
T (K)	293(2)
Crystal system	triclinic
Space group	$P\bar{1}$
Unit cell dimensions	
a (Å)	7.675(3)
b (Å)	8.805(3)
c (Å)	13.245(5)
α (°)	74.700(7)
β (°)	75.615(7)
γ (°)	70.012(7)
V (Å 3)	798.8(5)
Z	2
λ (Å)	0.71073
μ (Mo K α) (mm $^{-1}$)	2.001
D_{calc} (Mg m $^{-3}$)	1.697
Index range	$-9 \leq h \leq 9, -10 \leq k \leq 10, -15 \leq l \leq 15$
θ range (°)	1.62–25.00
Refine parameters	191
Total reflection	2806
Unique data [$I > 2\sigma(I)$]	2492
R_1^{a} [$I > 2\sigma(I)$]	0.0307
wR_2^{b}	0.0804
Goodness-of-fit	1.131
Δ_{max} (e Å $^{-3}$)	0.255
Δ_{min} (e Å $^{-3}$)	-0.517

^a $R = \sum |F_0 - F_c| / \sum F_0$.

^b $wR = [\sum w(F_0^2 - F_c^2) / \sum w F_0^4]^{1/2}$ are general but w are different, $w = 1 / [w^2(P^2) + (0.0360P)^2 + 0.2100P]$ where $P = (F_0^2 + 2F_c^2)/3$.

(7.7). ^1H NMR (300 MHz, CDCl_3), δ (ppm), (J (Hz)): 7.41 (bs, 4H), 7.24 (bs, 5H), 7.35 (d, 7.00 Hz, 8H), 7.44 (m, 9 and 10H), 8.10 (d, 8.00 Hz, 11H), 4.32 (s, 1-CH₃), 2.60 (s, S-CH₃). $[Zn(SMeaaiEt)(H_2O)Cl_2]$ (3b). Anal. Calc. for $ZnC_{12}H_{16}N_4OSCl_2$: C, 35.97; H, 3.99; N, 13.99. Found: C, 35.91; H, 4.03; N, 13.92%. FT-IR (KBr disc, cm^{-1}): $\nu(\text{N}=\text{N})$, 1429; $\nu(\text{C}=\text{N})$, 1624. UV-Vis spectroscopic data in CH_3CN (λ_{\max} (nm) ($10^{-3} \epsilon$ ($\text{dm}^3 \text{mol}^{-1} \text{cm}^{-1}$))): 363 (14.76), 417 (9.9). ^1H NMR (300 MHz, CDCl_3), δ (ppm), (J (Hz)): 7.42 (bs, 4H), 7.23 (bs, 5H), 7.32 (d, 7.00 Hz, 8H), 7.43 (m, 9 and 10H), 7.98 (d, 8.00 Hz, 11H), 4.48 (q, 6.60 Hz, 1-CH₂), 1.65 (t, 7.30 Hz, (1-CH₂)-CH₃), 2.67 (s, S-CH₃). $[Zn(SEtaaiMe)(H_2O)Cl_2]$ (3c). Anal. Calc. for $ZnC_{12}H_{16}N_4OSCl_2$: C, 35.97; H, 3.99; N, 13.99. Found: C, 35.94; H, 4.02; N, 13.97%. FT-IR (KBr disc, cm^{-1}): $\nu(\text{N}=\text{N})$, 1428; $\nu(\text{C}=\text{N})$, 1623. UV-Vis spectroscopic data in CH_3CN (λ_{\max} (nm) ($10^{-3} \epsilon$ ($\text{dm}^3 \text{mol}^{-1} \text{cm}^{-1}$))): 364 (12.3), 417 (10). ^1H NMR (300 MHz, CDCl_3), δ (ppm), (J (Hz)): 7.40 (bs, 4H), 7.23 (bs, 5H), 7.34 (d, 7.40 Hz, 8H), 7.46 (m, 9 and 10H), 7.94 (d, 7.90 Hz, 11H), 4.28 (s, 1-CH₃), 3.01 (q, 7.20 Hz, S-CH₂), 1.31 (t, 7.35 Hz, (S-CH₂)-CH₃). $[Zn(SEtaaiNet)(H_2O)Cl_2]$ (3d). Anal. Calc. for $ZnC_{13}H_{18}N_4OSCl_2$: C, 37.65; H, 4.34; N, 13.52. Found: C, 37.72; H, 4.38; N, 15.49%. FT-IR (KBr disc, cm^{-1}): $\nu(\text{N}=\text{N})$, 1430; $\nu(\text{C}=\text{N})$, 1623. UV-Vis spectroscopic data in CH_3CN (λ_{\max} (nm) ($10^{-3} \epsilon$ ($\text{dm}^3 \text{mol}^{-1} \text{cm}^{-1}$))): 363 (13.87), 415 (10.8). ^1H NMR (300 MHz, CDCl_3), δ (ppm), (J (Hz)): 7.41 (bs, 4H), 7.22 (bs, 5H), 7.35 (d, 7.00 Hz, 8H), 7.45 (m, 9 and 10H), 7.97 (d, 8.00 Hz, 11H), 4.59 (q, 6.70 Hz, 1-CH₂), 1.60 (t, 7.20 Hz, (1-CH₂)-CH₃), 3.04 (q, 7.20 Hz, S-CH₂), 1.39 (t, 7.36 Hz, (S-CH₂)-CH₃).

$[Zn(SMeaaiNMe)(H_2O)Br_2]$ (4a). Anal. Calc. for $C_{11}H_{14}N_4OSBr_2Zn$: C, 27.78; H, 2.95; N, 11.79. Found: C, 27.72; H, 2.92; N, 11.84%. FT-IR (KBr disc, cm^{-1}): $\nu(\text{N}=\text{N})$, 1423; $\nu(\text{C}=\text{N})$, 1612. UV-Vis spectroscopic data in CH_3CN (λ_{\max} (nm) ($10^{-3} \epsilon$ ($\text{dm}^3 \text{mol}^{-1} \text{cm}^{-1}$))): 363 (10.84), 417 (6.9). ^1H NMR (300 MHz, CDCl_3), δ (ppm), (J (Hz)): 7.40 (bs, 4H), 7.23 (bs, 5H), 7.36 (d, 7.40 Hz, 11H), 7.55 (m, 9 and 10H), 7.84 (d, 8.00 Hz), 4.72 (s, 1-CH₃), 2.55 (s, S-CH₃). $[Zn(SMeaaiNet)(H_2O)Br_2]$ (4b). Anal. Calc. for $C_{12}H_{16}N_4OSBr_2Zn$: C, 29.44; H, 3.27; N, 11.45. Found: C, 29.37; H, 3.32; N, 11.52%. FT-IR (KBr disc, cm^{-1}): $\nu(\text{N}=\text{N})$, 1424; $\nu(\text{C}=\text{N})$, 1610. UV-Vis spectroscopic data in CH_3CN (λ_{\max} (nm) ($10^{-3} \epsilon$ ($\text{dm}^3 \text{mol}^{-1} \text{cm}^{-1}$))): 365 (14.81), 417 (9.78). ^1H NMR (300 MHz, CDCl_3), δ (ppm), (J (Hz)): 7.41 (bs, 4H), 7.20 (bs, 5H), 7.33 (d, 7.00 Hz, 8H), 7.52 (m, 9 and 10H), 7.88 (d, 8.00 Hz, 11H), 4.47 (q, 7.00 Hz, 1-CH₂), 1.69 (t, 7.30 Hz, (1-CH₂)-CH₃), 2.64 (s, S-CH₃). $[Zn(SEtaaiNMe)(H_2O)Br_2]$ (4c). Anal. Calc. for $C_{12}H_{16}N_4OSBr_2Zn$: C, 29.44; H, 3.27; N, 11.45. Found: C, 29.50; H, 3.23; N, 11.53%. FT-IR (KBr disc, cm^{-1}): $\nu(\text{N}=\text{N})$, 1425; $\nu(\text{C}=\text{N})$, 1611. UV-Vis spectroscopic data in CH_3CN (λ_{\max} (nm) ($10^{-3} \epsilon$ ($\text{dm}^3 \text{mol}^{-1} \text{cm}^{-1}$))): 364 (13.12), 418 (9.88). ^1H



(i) Imidazole, pH 7; (ii) NaH in THF and R'I

$[Zn(SRaaiNR')(H_2O)X_2]$ (X = Cl (3), Br (4), I (5)) [$R = R' = \text{Me}$ (a); $R = \text{Me}$, $R' = \text{Et}$ (b);

$R = \text{Et}$, $R' = \text{Me}$ (c); $R = R' = \text{Et}$ (d)]

Scheme 1. The ligands and the complexes.

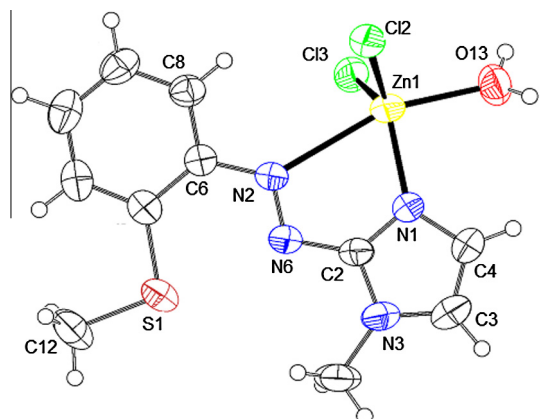


Fig. 1. Molecular structure of $[Zn(SMeaaINMe)(H_2O)Cl_2]$ (**3a**).

Table 2
Selected bond distances and bond angles of $[Zn(SMeaaINMe)(H_2O)Cl_2]$ (**3a**).

Bond lengths (Å)		Bond angles (°)	
Zn(1)–N(1)	2.007(2)	N(1)–Zn(1)–O(13)	92.36(9)
Zn(1)–N(2)	2.608(6)	N(1)–Zn(1)–N(2)	69.88(3)
Zn(1)–O(13)	2.130(2)	N(1)–Zn(1)–Cl(2)	119.99(7)
Zn(1)–Cl(2)	2.2442(10)	N(1)–Zn(1)–Cl(3)	118.32(7)
Zn(1)–Cl(3)	2.2445(11)	O(13)–Zn(1)–Cl(2)	98.75(8)
N(2)–N(6)	1.269(3)	O(13)–Zn(1)–Cl(3)	96.05(8)
N(2)–C(6)	1.399(3)	Cl(2)–Zn(1)–Cl(3)	118.74(3)
		N(2)–Zn(1)–Cl(2)	94.56(2)
		N(2)–Zn(1)–Cl(3)	88.57(4)
		N(2)–Zn(1)–O(13)	169.31(4)

NMR (300 MHz, $CDCl_3$), δ (ppm), (J (Hz)): 7.42 (bs, 4H), 7.20 (bs, 5H), 7.35 (d, 7.00 Hz, 8H), 7.56 (m, 9 and 10H), 7.83 (d, 8.00 Hz, 11H), 4.30 (s, 1-CH₃), 3.00 (q, 7.40 Hz, S-CH₂), 1.30 (6.20 Hz, (S-CH₂)-CH₃). $[Zn(SEtaaiNET)(H_2O)Br_2]$ (**4d**). *Anal.* Calc. for $C_{13}H_{18}N_4OSBr_2Zn$: C, 31.01; H, 3.58; N, 11.13. Found: C, 31.00; H, 3.60; N, 11.18%. FT-IR (KBr disc, cm^{-1}): $\nu(N=N)$, 1426; $\nu(C=N)$, 1614. UV-Vis spectroscopic data in CH_3CN (λ_{max} (nm) ($10^{-3} \epsilon$ ($dm^3 mol^{-1} cm^{-1}$))): 363 (13.52), 419 (10.2). ¹H NMR (300 MHz, $CDCl_3$), δ (ppm), (J (Hz)): 7.41 (bs, 4H), 7.22 (bs, 5H), 7.32 (d, 7.00 Hz, 7.53 (m, 9 and 10-), 7.86 (d, 8.00 Hz, 11H), 4.52 (q, 7.25 Hz, 1-CH₂), 1.62 (t, 7.20 Hz, (1-CH₂)-CH₃), 3.04 (q, 7.30 Hz, S-CH₂), 1.35 (t, 6.20 Hz, (S-CH₂)-CH₃). $[Zn(SMeaaINMe)(H_2O)I_2]$ (**5a**). *Anal.* Calc. for $C_{11}H_{14}N_4OSI_2Zn$: C, 23.19; H, 2.46; N, 9.84. Found: C, 23.23; H, 2.50; N, 9.80%. FT-IR (KBr disc, cm^{-1}): $\nu(N=N)$, 1424; $\nu(C=N)$, 1601. UV-Vis spectroscopic data in CH_3CN (λ_{max} (nm) ($10^{-3} \epsilon$ ($dm^3 mol^{-1} cm^{-1}$))): 364 (9.65), 415 (6.23). ¹H NMR (300 MHz, $CDCl_3$), δ (ppm), (J (Hz)): 7.41 (bs, 4H), 7.28 (bs, 5H), 7.31 (d, 7.00 Hz, 8H), 7.55 (m, 9 and 10H), 7.80 (d, 8.00 Hz, 11H), 4.14 (s, 1-CH₃), 2.52 (s, S-CH₃). $[Zn(SMeaaINET)(H_2O)I_2]$ (**5b**). *Anal.* Calc. for $C_{12}H_{16}N_4OSI_2Zn$: C, 24.70; H, 2.74; N, 9.60. Found: C, 24.74; H, 2.71; N, 9.66%. FT-IR (KBr disc, cm^{-1}): $\nu(N=N)$, 1428; $\nu(C=N)$, 1605. UV-Vis spectroscopic data in CH_3CN (λ_{max} (nm) ($10^{-3} \epsilon$ ($dm^3 mol^{-1} cm^{-1}$))): 365 (14.81), 419 (9.64). ¹H NMR (300 MHz, $CDCl_3$), δ (ppm), (J (Hz)): 7.40 (bs, 4H), 7.23 (bs, 5H), 7.34 (d, 7.00 Hz, 8H), 7.56 (m, 9 and 10H), 7.82 (d, 8.00 Hz, 11H), 4.51 (q, 7.00 Hz, 1-CH₂), 1.63 (t, 7.30 Hz, (1-CH₂)-CH₃), 2.59 (s, S-CH₃). $[Zn(SEtaaiNMe)(H_2O)I_2]$ (**5c**). *Anal.* Calc. $C_{12}H_{16}N_4OSI_2Zn$: C, 24.70; H, 2.74; N, 9.60. Found: C, 24.67; H, 2.79; N, 9.63%. FT-IR (KBr disc, cm^{-1}): $\nu(N=N)$, 1426; $\nu(C=N)$, 1604. UV-Vis spectroscopic data in CH_3CN (λ_{max} (nm) ($10^{-3} \epsilon$ ($dm^3 mol^{-1} cm^{-1}$))): 363 (13.55), 418 (9.71). ¹H NMR (300 MHz, $CDCl_3$), δ (ppm),

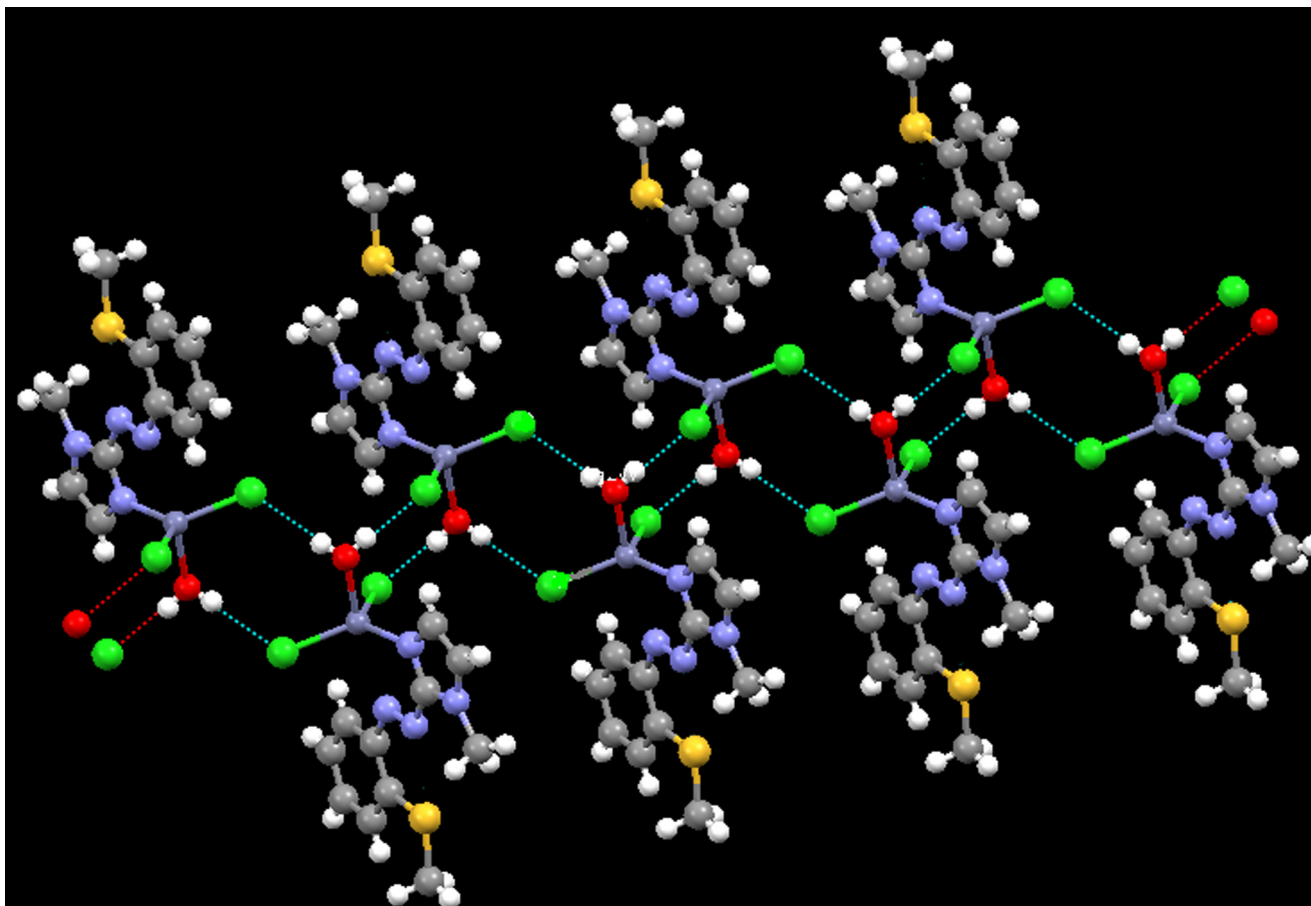


Fig. 2. 1D chain constituted by O-H...Cl bonds with neighboring molecules.

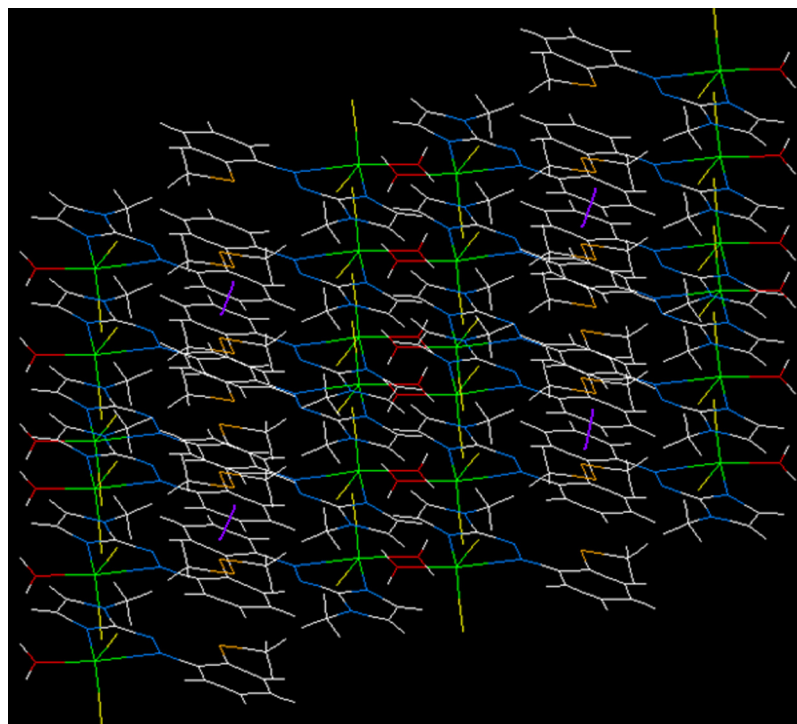
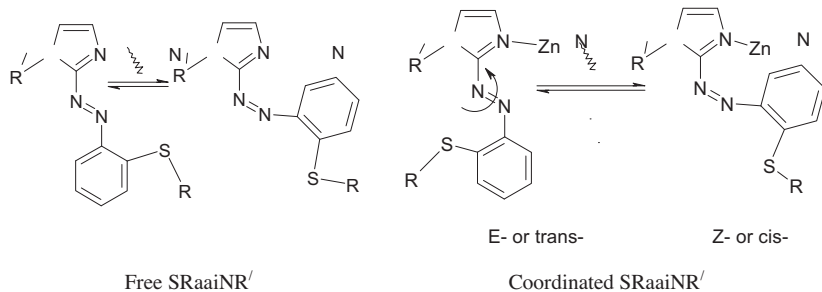


Fig. 3. Formation of a 2D supramolecular plane via $\text{Cg}(3)\cdots\text{Cg}(3)$ interactions (/ $\text{Cg}(3)$):



Scheme 2. Photochromism of free SRaaiNR' and the coordinated ligand in $[\text{Zn}(\text{SRaaiNR}')(\text{H}_2\text{O})\text{Cl}_2]$.

(J (Hz)): 7.43 (bs, 4H), 7.27 (bs, 5H), 7.32 (d, 7.40 Hz, 8H), 7.55 (m, 9 and 10H), 7.81 (d, 8.00 Hz, 11H), 4.17 (s, 1-CH₃), 3.00 (q, 7.30 Hz, S-CH₂), 1.29 (t, 7.00 Hz, (S-CH₂)-CH₃). $[\text{Zn}(\text{SEtaaiNEt})(\text{H}_2\text{O})_2]$ (**5d**). *Anal.* Calc. for $\text{C}_{13}\text{H}_{18}\text{N}_4\text{OSBr}_2\text{Zn}$: C, 26.13; H, 3.01; N, 9.38. Found: C, 26.10; H, 3.05; N, 9.42%. FT-IR (KBr disc, cm⁻¹): $\nu(\text{N}=\text{N})$, 1427; $\nu(\text{C}=\text{N})$, 1605. UV-Vis spectroscopic data in CH_3CN (λ_{max} (nm) (10^{-3} \in ($\text{dm}^3 \text{ mol}^{-1} \text{ cm}^{-1}$))): 364 (13.68), 417 (9.8). ¹H NMR (300 MHz, CDCl_3), δ (ppm), (J (Hz)): 7.42 (bs, 4H), 7.22 (bs, 5H), 7.33 (d, 7.00 Hz, 8H), 7.56 (m, 9 and 10H), 7.80 (d, 8.00 Hz, 11H), 4.44 (q, 7.30 Hz, 1-CH₂), 1.61 (t, 7.30 Hz, (1-CH₂)-CH₃), 3.05 (q, 7.40 Hz, S-CH₂), 1.30 (t, 5.30 Hz, (S-CH₂)-CH₃) (bs, broad singlet; s, singlet; d, doublet; t, triplet; q, quintet; m, multiplet).

2.4. X-ray diffraction study

Single crystals suitable for X-ray diffraction data collection were grown from slow evaporation of the complexes in methanol. The crystal data are given in Table 1. A suitable single crystal of $[\text{Zn}(\text{SMeaaiMe})(\text{H}_2\text{O})\text{Cl}_2]$ (**3a**) ($0.26 \times 0.24 \times 0.22$ mm) was mounted on a Bruker SMART APEX CCD diffractometer and data were collected by the use of ω scans. Unit cell parameters were determined from least-squares refinement. Data were corrected for Lorentz polarization effects and for linear decay. Semi-empirical

cal absorption corrections based on ψ -scans were applied. The structures were solved by the direct method using SHELXS-97 [28] and successive difference Fourier syntheses. All non-hydrogen atoms were refined anisotropically. The hydrogen atoms were fixed geometrically and refined using the riding model. All calculations were carried out using the SHELXL-97 [29], PLATON-99 [30] and ORTEP-32 [31] programs.

2.5. Photometric measurements

Absorption spectra were taken with a PerkinElmer Lambda 25 UV-Vis spectrophotometer in a 1×1 cm quartz optical cell maintained at 25 °C with a Peltier thermostat. The light source of a PerkinElmer LS 55 spectrofluorimeter was used as an excitation light, with a slit width of 10 nm. An optical filter was used to cut off overtones when necessary. Upon UV light irradiation at λ_{max} of the $\pi\pi^*$ absorption to a solution of the complex, the intense $\pi\pi^*$ peak decreases, which is accompanied by a slight increase at the tail portion of the spectrum around 450 nm ($n\pi^*$) until a photostationary state (PSS-I) is reached. Subsequent irradiation at the newly appeared longer wavelength peak ($n\pi^*$) reverses the course of the reaction and the original spectrum is recovered up to a point, which is another photostationary state (PSS-II) under $n\pi^*$

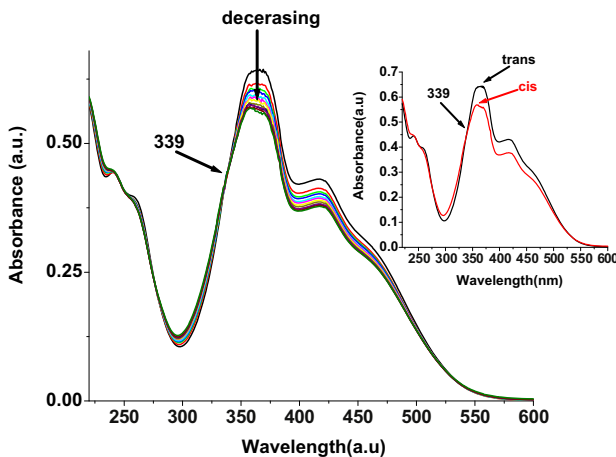


Fig. 4. Photochromism of $[Zn(SMeaiNET)(H_2O)Cl_2]$ (**3b**), E \rightarrow Z isomerisation in CH_3CN at $25^\circ C$.

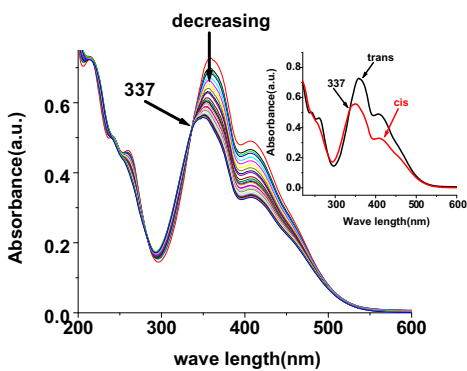


Fig. 5. Photochromism of SMeaiNET (**2b**) in CH_3CN at $25^\circ C$.

irradiation. An isosbestic point at 335–340 nm is reached during this process. The absorption spectra of the cis isomers were obtained by extrapolation of the absorption spectra of a cis-rich mixture for which the composition is known from 1H NMR integration. Quantum yields (ϕ) were obtained by measuring the initial E-to-Z isomerization rates (v) in a well-stirred solution within the above instrument using the equation:

Table 3
Excitation wavelength ($\lambda_{\pi\pi^*}$), rate of E \rightarrow Z conversion and quantum yield ($\Phi_{E \rightarrow Z}$).

Compound	$\lambda_{\pi\pi^*}$ (nm)	Isosbestic points (nm)	Rate of E \rightarrow Z conversion $\times 10^8$ (s^{-1})	$\Phi_{E \rightarrow Z}$
SMeaiNMe (2a) [#]	357	337	4.908	0.317
SMeaiNET (2b) [#]	358	337	3.108	0.232
SEtaaiNMe (2c) [#]	357	336	4.67	0.290
SEtaaiNET (2d) [#]	356	335	2.948	0.1974
$[Zn(SMeaiNMe)(H_2O)Cl_2]$ (3a)	362	339	2.88	0.161
$[Zn(SEtaaiNMe)(H_2O)Cl_2]$ (3b)	363	339	2.33	0.1305
$[Zn(SMeaiNET)(H_2O)Cl_2]$ (3c)	362	338	2.45	0.142
$[Zn(SEtaaiNET)(H_2O)Cl_2]$ (3d)	361	337	1.89	0.0913
$[Zn(SMeaiNMe)(H_2O)Br_2]$ (4a)	363	338	3.22	0.179
$[Zn(SEtaaiNMe)(H_2O)Br_2]$ (4b)	362	337	2.68	0.148
$[Zn(SMeaiNET)(H_2O)Br_2]$ (4c)	364	337	2.77	0.155
$[Zn(SEtaaiNET)(H_2O)Br_2]$ (4d)	363	339	2.03	0.105
$[Zn(SMeaaNMe)(H_2O)_2]$ (5a)	364	337	3.65	0.231
$[Zn(SEtaaiNMe)(H_2O)_2]$ (5b)	365	338	3.05	0.159
$[Zn(SMeaiNET)(H_2O)_2]$ (5c)	363	336	3.18	0.164
$[Zn(SEtaaiNET)(H_2O)_2]$ (5d)	364	337	2.21	0.121

[#] Ref. [26].

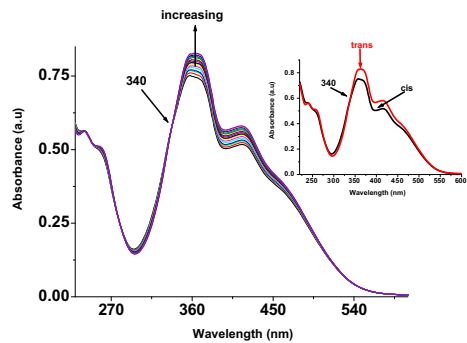


Fig. 6. Z \rightarrow E isomerisation of $[Zn(SMeaiNET)(H_2O)Cl_2]$ in $MeCN$ at 303 K .

$$v = (\phi I_0/V) (1 - 10^{-Abs})$$

where I_0 is the photon flux at the front of the cell, V is the volume of the solution and Abs is the initial absorbance at the irradiation wavelength. The value of I_0 was obtained by using azobenzene ($\phi = 0.11$ for $\pi-\pi^*$ excitation [32]) under the same irradiation conditions.

The thermal rates of Z-to-E isomerisation were obtained by monitoring absorption changes intermittently for a cis-rich solution kept in the dark at constant temperatures (T) in the range 298–321 K. The activation energy (E_a) and the frequency factor (A) were obtained from the Arrhenius plot:

$$\ln k = \ln A - E_a/RT$$

where k is the measured rate constant, R is the gas constant and T is temperature. The values of the activation free energy (ΔG^*) and activation entropy (ΔS^*) were obtained through the relationships,

$$\Delta G^* = E_a - RT - T\Delta S^*/and/\Delta S^* = [\ln A - 1 - \ln(k_B T/h)/R]$$

where k_B and h are Boltzmann's and Plank's constants

3. Results and discussion

3.1. The formulation of the complexes

1-Alkyl-2-[(o-thioalkyl)phenylazo]imidazoles [SRaaNR' (R = R' = Me (**2a**); R = Me, R' = Et (**2b**); R = Et, R' = Me (**2c**); R = R' = Et (**2d**)] have been reacted with anhydrous ZnX_2 (X = Cl, Br, I) in methanol, and orange-red crystalline compounds $[Zn(SRaaiNR')(H_2O)X_2]$

Table 4Rate and activation parameters for E → Z thermal isomerisation of [Zn(SRaaiNR')(H₂O)Cl₂] (**3–5**).

Compd	Temp (K)	Rate of thermal E → Z conversion × 10 ⁴ (s ⁻¹)	E _a (kJ mol ⁻¹)	ΔH [*] (kJ mol ⁻¹)	ΔS [*] (J mol ⁻¹ K ⁻¹)	ΔG [*] (kJ mol ⁻¹)
2a [§]	298	4.329	25.42	22.88	−232.41	92.13
	303	5.295				93.29
	308	6.191				94.45
	313	7.091				95.62
2b [§]	298	4.614	22.99	20.45	−240.02	91.97
	303	5.598				93.17
	308	6.293				94.37
	313	7.269				95.57
2c [§]	298	4.425	21.92	19.38	−244.04	92.11
	303	5.123				93.33
	308	5.985				94.55
	313	6.729				95.77
2d [§]	298	4.625	18.88	16.34	−253.96	92.02
	303	5.123				93.29
	308	5.985				94.56
	313	6.589				95.83
3a	303	5.67	17.18	14.60	−259.14	78.53
	308	6.063				79.83
	313	6.857				81.13
	318	7.812				82.42
3b	303	5.875	15.95	13.37	−262.90	79.67
	308	6.263				80.99
	313	6.975				82.30
	318	7.905				83.61
3c	303	5.921	15.60	13.017	−263.97	79.99
	308	6.363				81.31
	313	7.101				82.63
	318	7.9				83.95
3d	303	6.18	13.67	11.09	−270.00	81.82
	308	6.51				83.17
	313	7.19				84.52
	318	7.95				85.87
4a	303	5.811	18.31	15.73	−255.22	77.34
	308	6.251				78.62
	313	7.222				79.9
	318	8.11				81.17
4b	303	5.991	17.47	14.89	−257.76	78.12
	308	6.401				79.40
	313	7.332				80.69
	318	8.24				81.98
4c	303	6.111	17.53	14.95	−257.40	78.01
	308	6.483				79.29
	313	7.484				80.58
	318	8.395				81.87
4d	303	6.288	14.18	11.60	−268.19	81.27
	308	6.612				82.62
	313	7.348				83.96
	318	8.159				85.30
5a	303	5.901	19.41	16.83	−251.50	76.22
	308	6.309				77.48
	313	7.441				78.74
	318	8.369				79.99
5b	303	6.051	18.16	15.58	−255.39	77.40
	308	6.474				78.68
	313	7.5				79.95
	318	8.411				81.23
5c	303	6.11	18.40	15.82	−254.51	77.13
	308	6.508				78.41
	313	7.591				79.68
	318	8.518				80.95
5d	303	6.409	15.76	13.18	−262.81	79.64
	308	6.823				80.96
	313	7.618				82.27
	318	8.581				83.59

[§] Received from Ref. [26].

have been isolated. Microanalytical data has confirmed the composition of the complexes. Thermal studies of the complexes show one step elimination of H_2O within temperature range 105–140 °C, which supports the coordination of H_2O to Zn(II). The complexes are stable up to 245 °C.

The infrared spectra of the complexes show moderately intense stretching vibrations at 1609–1625 and 1419–1430 cm⁻¹, which are assigned to $\nu(\text{C}=\text{N})$ and $\nu(\text{N}=\text{N})$ by comparing with published work [26,27]. The ¹H-NMR spectra of the complexes are recorded in CDCl₃ and the signals are assigned unambiguously via spin–spin interactions, the effect of substitutions therein and on comparing with free ligand data [26,27]. The atom numbering pattern is shown in the Scheme 1. Imidazolyl 4 and 5H show a broad singlet at 7.4 and 7.2 ppm, respectively for the complexes [Zn(SRaaiNR')(H₂O)X₂] (**3–5**) and these are downfield shifted by 0.1–0.2 ppm compared to the free ligand data. The broadening may be due to rapid proton exchange between these imidazolyl protons and/or exchange with solvent protons. The phenyl protons (8 to 11H) of –S-(R)-C₆H₄ remain almost unperturbed. This spectral information supports the single crystal structure (Fig. 1), where SMeaaiNMe acts as a bidentate imidazolyl-N and azo-N chelating agent. The N(1)-Me peak appears as a singlet at ca. 4.2 ppm; N-CH₂-CH₃ shows a quartet for –CH₂– at ca. 4.5 (7 Hz) and a triplet at ca. 1.6 (7 Hz) ppm. The thioalkyl group S-R also exhibits a singlet signal at 2.6 ppm for S-Me of SMeaaiNR' (**3a,b–6a,b**). SEtaai-NET (**3d–6d**) shows two quartets at 4.5 (7 Hz) and 3.00 (7 Hz) ppm for –CH₂– protons of N-CH₂-(CH₃) and S-CH₂-(CH₃), respectively and two triplets at 1.6 (7 Hz) and 1.3 (6 Hz) ppm for -(N-CH₂)-CH₃ and -(S-CH₂)-CH₃, respectively.

3.2. Molecular structure of Zn(SMeaaiNMe)(H₂O)Cl₂] (**3a**)

The crystal structure of [Zn(SMeaaiNMe)(H₂O)Cl₂] (**3a**) is given in Fig. 1 and bond parameters are listed in Table 2. The ligand, SMeaaiNMe has three potential donor centres – N(imidazolyl), N(azo) and S(Me), while it shows, in this example, bidentate N(imidazolyl) and N(azo) chelation. The --- unit has a Zn-N(azo) distance of 2.608(6) Å, which is longer than previously reported data, e.g. 2.546(3) Å for [Zn(MeaaiMe)(H₂O)Cl₂] (MeaaiMe = 1-methyl-2-(*p*-tolylazo)imidazole) [18], but shorter than the sum of the van der Waals radii of Zn(II) (1.39 Å) and N(sp²) (1.55 Å). The chelate angle is 69.88(3)° and this is comparable to the reported data in a series of chelated arylazoimidazole complexes [14,15,18,19,26]. The angles in the coordination sphere are Cl(2)-Zn(1)-Cl(3), 118.74(3)°; N(1)-Zn(1)-Cl(2), 119.99(7)°; N(1)-Zn(1)-Cl(3), 118.32(7)° and τ = 0.70, which imply a five coordinated distorted square pyramidal geometry about Zn(II) [33]. The distorted square plane is constituted by Zn(1), N(1), N(2), Cl(3) and O(13); Cl(2) is assumed to be in the apical position of the square pyramid. Two aromatic rings attached to –N=N–, imidazolyl and thiophenyl make a dihedral angle of 5.19(10)°. The N=N bond length is 1.269(3) Å and this is slightly elongated compared to that of the free ligand value (1.250(1) Å) [17]. The two Zn-Cl bonds are almost equal in length, Zn-Cl(2), 2.2442(10) and Zn-Cl(3), 2.2445(11) Å, and they are longer than related reported distances (2.223(1) and 2.256(1) Å) [15].

The coordinated H₂O-Zn unit shows two hydrogen bonds, Zn-O(HA)-HB···Cl(2) and Zn-O(HB)-HA···Cl(3), with two adjacent molecules and this is the reason for an infinite 1D chain (Fig. 2); and $\pi\cdots\pi$ interactions between thiophenyl rings of adjacent molecules constitute a 2D structure (Fig. 3). One of the two O-H bonds of H₂O interacts with Cl (Zn–Cl bonds) of adjacent molecules, (Zn)Cl(2/2A)···H(O)H···Cl(3/3A)(Zn) (Cl(2/2A)···H-O, d(O···Cl(2/2A)), 3.18(6); d(H···Cl(2/2A)), 2.36(7) Å and \angle O-H···Cl, 170.9(3)°, to construct a 1D chain (symmetry 2 – x , 2 – y , 1 – z for Cl(2) and 1 – x , 2 – y , 1 – z for Cl(3)). The coordinated H₂O of one

molecule in a row interacts via hydrogen bonding with two adjacent molecules [(Zn)Cl(2)···H(O)H···Cl(2A)(Zn) ...] of a second row and vice versa. Two hydrogen bonds, Zn–O(H)-H···Cl(2/3), make eight member supracycles and form hydrogen bonding with adjacent units, leading to the formation of 1D chain. The pendant thiophenyl ring (C(6)-C(7)-C(8)-C(9)-C(10)-C(11)) in each row shows a $\pi\cdots\pi$ interaction with the same ring of an adjacent layer (3.639(2) Å and symmetry 1 – x , 1 – y , 2 – z) to constitute a 2D network (Fig. 3).

3.3. UV-Vis spectra and photochromism

The solution electronic spectra of the compounds were recorded in CH₃CN in the range 200–600 nm. There are two bands in the UV-Vis region at 360–380 and 410–420 nm. On comparing with the spectra of the free ligands [27] and that of Zn(II) complexes, we may conclude that these bands come from intramolecular charge-transfer transitions ($n \rightarrow \pi^*$, $\pi \rightarrow \pi^*$).

The E-to-Z (*trans*-to-*cis*) isomerisation of the complexes (Scheme 2) has been investigated by irradiation of UV light in acetonitrile solution (Fig. 4) and compared with free ligand spectral changes (Fig. 5). The absorption spectra of the E-configuration of the coordinated SRaaiNR' ligand in complexes **3–5** in CH₃CN show a gradual decrease in absorbance at 350–355 nm and an increase in absorbance at 245–255 nm, and an isosbestic point is assigned at 335–340 nm. The complexes show little degradation upon repeated irradiation of at least up to 15 cycles in each case, which has been verified by measuring the absorbance before and after irradiation at the $\pi \rightarrow \pi^*$ band. The quantum yields were measured for the E-to-Z ($\Phi_{E \rightarrow Z}$) photoisomerisation of these compounds in CH₃CN on irradiation with UV light (Table 3). The $\Phi_{E \rightarrow Z}$ values are significantly dependent on the nature of the substituents, halide type and molecular weight [18,19,26,34–36]. In the presence of 1-Me and 1-Et groups, the quantum yield is reduced in the complexes compared to the free ligand.

Upon UV light irradiation, the E structure of SRaaiNR' changes to the Z structure about the azo (–N=N–) function and the Z molar ratio reached >80% (Scheme 2). This technique may assist the rotation of the azo-aryl group (–N=N–Ar), which isomerizes from the E to Z structure. The rates of photoisomerisation increase with decreasing electronegativity of X in the complexes (Table 3); the rate follows [Zn(SRaaiNR')Cl₂] (**3**) < [Zn(SRaaiNR')Br₂] (**4**) < [Zn(SRaaiNR')I₂] (**5**), although the molar mass follows the order **3** < **4** < **5**. The higher electronegativity of Cl in **3** may help to enhance the association strength with neighboring molecules and may effectively increase the rotor mass to more than that of **4** or **5**. The molecular association has been supported in the crystalline state by hydrogen bonds and $\pi\cdots\pi$ interactions (*vide supra*).

The thermal Z-to-E isomerisation of the complexes was followed by UV-Vis spectroscopy (Fig. 6) in MeCN at various

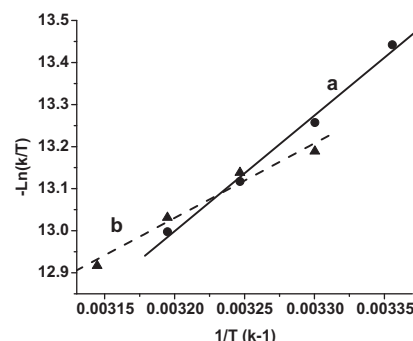


Fig. 7. Arrhenius plots of Z-to-E thermal isomerisation of (a) SMeaaiNMe (**2a**) (■, --) and (b) [Zn(SMeaaiNMe)(H₂O)Cl₂] (▲, - –) (**3a**) at various temperatures (303–318 K).

temperatures in the range 303–318 K, and the activation energies were obtained (Table 4) from Arrhenius plots (Fig. 7). In the complexes, the E_a s are less than that of the free ligands, which mean a slow rate of Z-to-E thermal isomerisation of the complexes. The entropies of activation (ΔS^*) are more negative in the complexes than for the free ligands. This also defends the increase in rotor volume in the complexes.

4. Conclusion

$[Zn(SRaaiNR')(H_2O)X_2]$ ($SRaaiNR'$ = 1-alkyl-2- $\{(o\text{-thioalkyl})\text{phenylazo}\}$ imidazole; $X = \text{Cl}, \text{Br}, \text{I}$) are pentacoordinated distorted square pyramidal complexes. UV light irradiation to a solution of the complexes causes photoisomerisation, E (*trans*) \leftrightarrow Z (*cis*) about $-\text{N}=\text{N}-$ of SRaaiNR'. The decrease in electronegativity of X increases the rate of E-to-Z photoisomerisation. The rates and quantum yields of isomerisation are regulated by the rotor mass and volume of the photochrome – complexes of a higher rotor mass and volume commonly show slower rates of isomerisation. The Z-to-E isomerisation is a thermal process and the activation energies (E_a) are reduced to 50–60% of the free ligand values.

Acknowledgments

Financial support from Department of Science & Technology, New Delhi is thankfully acknowledged.

Appendix Supplementary. material

CCDC 948112; contains the supplementary crystallographic data for $Zn(SMeaaiNMe)(H_2O)\text{Cl}_2$ [3a]. These data can be obtained free of charge via <http://www.ccdc.cam.ac.uk/conts/retrieving.html>, or from the Cambridge Crystallographic Data Centre, 12 Union Road, Cambridge CB2 1EZ, UK; fax: (+44) 1223-336-033; or e-mail: deposit@ccdc.cam.ac.uk.

References

- [1] F.A. Cotton, G. Wilkinson, Advanced Inorganic Chemistry, fifth ed., John Wiley & Sons, New York, 1988.
- [2] W. Kaim, B. Schwederski, Bio-Inorganic Chemistry. Inorganic Elements in the of Life, Wiley, New York, 1994.
- [3] H. Eklund, C.-I. Branden, in: T.G. Spiro (Ed.), Zinc Enzymes, Wiley, New York, 1983.
- [4] J.E. Fergusson, The Heavy Elements: Chemistry, Environmental Impact and Health Effects, Pergamon, Oxford, 1990.
- [5] R.C. van Landschoot, J.A.M. van Hest, J. Reedijk, Inorg. Chim. Acta 72 (1983) 89.
- [6] M.S. Nair, K. Venkatachalamapathi, M. Santappa, J. Chem. Soc., Dalton Trans. (1982) 555.
- [7] C.H. Wei, K.B. Jacobson, Inorg. Chem. 20 (1981) 356.
- [8] T.K. Misra, D. Das, C. Sinha, Polyhedron 16 (1997) 4163.
- [9] D. Mallick, A. Nandi, S. Datta, K.K. Sarker, T.K. Mondal, C. Sinha, Polyhedron 31 (2012) 506.
- [10] G. Saha, P. Datta, K.K. Sarker, R. Saha, G. Mostafa, C. Sinha, Polyhedron 30 (2011) 614.
- [11] P. Datta, D. Sardar, P. Mitra, C. Sinha, Polyhedron 30 (2011) 1516.
- [12] T.K. Mondal, P. Raghavaiah, A.K. Patra, C. Sinha, Inorg. Chem. Commun. 13 (2010) 273.
- [13] D. Das, A.K. Das, C. Sinha, Talanta 48 (1999) 1013.
- [14] J.K. Nag, P.K. Santra, C. Sinha, F.-L. Liao, T.-H. Lu, Polyhedron 20 (2001) 2253.
- [15] B.G. Chand, U.S. Ray, J. Cheng, T.-H. Lu, C. Sinha, Polyhedron 22 (2003) 1213.
- [16] D. Das, B.G. Chand, K.K. Sarker, J. Dinda, C. Sinha, Polyhedron 25 (2006) 2333.
- [17] J. Otsuki, K. Suwa, K. Narutaki, C. Sinha, I. Yoshikawa, K. Araki, J. Phys. Chem. A 109 (2005) 8064.
- [18] K.K. Sarker, B.G. Chand, J. Cheng, T.-H. Lu, C. Sinha, Inorg. Chem. 46 (2007) 670.
- [19] K.K. Sarker, D. Sardar, K. Suwa, J. Otsuki, C. Sinha, Inorg. Chem. 46 (2007) 8291.
- [20] K.K. Sarker, S. Saha Halder, D. Banerjee, T.K. Mondal, A.R. Paital, P.K. Nanda, P. Raghavaiah, C. Sinha, Inorg. Chim. Acta 363 (2010) 2955.
- [21] C.V. Yelamaggad, I. Shashikala, U.S. Hiremath, D.S.S. Rao, S.K. Prasad, Liq. Cryst. 34 (2007) 153.
- [22] S. Kawata, Y. Kawata, Chem. Rev. 100 (2000) 1777.
- [23] E. Katz, A.N. Shipway, I. Willner, in: Z. Sekkat, W. Knoll (Eds.), Photoreactive Organic Films, Academic, San Diego, 2002, p. 220.
- [24] M. Irie (Ed.), Special issue: Photochromism: Memories and Switches, Chem. Rev. 100 (2000) 1683.
- [25] J.C. Crano, R.J. Guglielmetti (Eds.), Organic Photochromic and Thermochromic Compounds, Kluwer Academic, Plenum Publishers, New York, NY, 1999.
- [26] S. Saha (Halder), P. Raghavaiah, C. Sinha, Polyhedron 46 (2012) 25.
- [27] D. Banerjee, U.S. Ray, S.K. Jasimuddin, J.-C. Liou, T.-H. Lu, C. Sinha, Polyhedron 25 (2006) 1299.
- [28] G.M. Sheldrick, SHELXS-97, Program for the Solution of Crystal Structure, University of Gottingen, Germany, 1997.
- [29] G.M. Sheldrick, SHELXL 97, Program for the Refinement of Crystal Structure, University of Gottingen, Germany, 1997.
- [30] A.L. Spek, PLATON, Molecular Geometry Program, University of Utrecht, The Netherlands, 1999.
- [31] L.J. Farrugia, J. Appl. Crystallogr. 30 (1997) 565.
- [32] G. Zimmerman, L. Chow, U. Paik, J. Am. Chem. Soc. 80 (1958) 3528.
- [33] A.W. Addison, T. Nageswara Rao, J. Chem. Soc., Dalton Trans. (1984) 1349.
- [34] D. Mallick, K.K. Sarker, P. Datta, T.K. Mondal, C. Sinha, Inorg. Chim. Acta 387 (2012) 352.
- [35] H. Nishihara, Bull. Chem. Soc. Jpn. 77 (2004) 407.
- [36] T. Yutaka, M. Kurihara, H. Nishihara, Mol. Cryst. Liq. Cryst. 343 (2000) 193.